ROBOTIC JOINT EXPERIMENTS UNDER ULTRAVACUUM

A. Borrien and L. Petitjean*

ABSTRACT

In the first part of the paper, various aspects of a robotic joint development program, including gearbox technology, electromechanical components, lubrication, and test results, are discussed.

A test prototype of the joint allowing simulation of robotic arm dynamic effects is presented in the second part of the paper. This prototype is tested under vacuum with different types of motors and sensors to characterize the functional parameters: angular position error, mechanical backlash, gearbox efficiency, and lifetime.

1. INTRODUCTION

The objectives of this paper are to present the gear technology, lubrication, and ultravacuum test results of a robotic joint with high Hertzian pressure on the gear teeth. Dynamic operation of the joint is studied to determine the influence of the control feedback law on significant parameters such as angular precision, speed variation, and damping rate of the joint. Finally, simulated lifetime results of the joint are discussed. After the ultravacuum lifetime test, mechanical and tribological reducer effects in the gearbox are examined to quantify wear level versus number of cycles.

2. JOINT DESIGN

2.1 General Specifications

Geometric, kinematic and dynamic specifications are based on system requirements established for accomplishing the mission with the manipulator arm.

General specifications are the following:

. Angular excursion	-90 deg to +90 deg
. Maximum output motor torque	10 Nm
. Holding output torque	60 Nm
. Global stiffness	7000 Nm/Rad.
. Maximum output backlash	2×10^{-3} Rad.
. Lifetime under ultravacuum	250 hours
. Vacuum level	10^{-8} torr
. Maximum output speed	5×10^{-2} Rad/sec

*Centre National d'Etudes Spatiales (CNES), Toulouse, France

2.2 Technological Definition

The electromechanical joint consists of a DC brushless motor, two optical encoders (input and output), a gearbox, and an electromechanical brake.

a) Motor

Our nominal choice consists of a space-qualified electrical DC brushless motor. The most important advantages are electronic and feedback law simplicity and good stability over a wide dynamic operating range as well as good steady state system performance. An alternative choice is based on a space-qualified stepper motor driven with a special control law. A standard mechanical interface allows comparison of the two alternatives with the same joint.

b) Sensor Modules

Two sensor configurations are possible for measuring joint parameters such as output angular position and input motor speed. System studies have shown that the angular speed of the joint must be sensed on the motor shaft and the angular position on the output housing to satisfy stability and damping criteria of the control loop.

c) Brake

A brake is placed on the motor shaft to latch the joint. A solenoid is energized to release the brake whenever the joint is to be driven.

d) Gear Transmission Description (see Figure 1)

Trade-off studies have concluded that the best solution consists of a parallel-axis back-driveable gearbox with several stages. The main advantages are:

- relatively simple manufacturing
- good potential efficiency
- low backlash
- gear geometry consistent with dry lubrication technology.

Gearbox Definition (see Figure 2). The reducer is divided into two kinematically symmetrical closed parallel branches which consist of:

- external spur gears for the first and second stage
- internal gear wheel for the output stage.

The objective of this design is to allow a fine adjustment of backlash and equal load sharing between the two branches.

- Gear material : 35NCD16 - Air hardened 875 deg C
  - Tempered 650 deg C
- Lubrication : PTFE coating

Geometric Characteristics

Stage	Module (mm)	Width	Teeth number	Gear ratio
1	0,5	3	20 120	6
2	0.7	7	17 86	5.06
3	1	9	17 103	6.06
Total ratio				183,90

Stage		Bending stress	Allowable bending stress	Hertzian Stress	Allowable Hertzian Stress
1	P	7.3	48.8	52.3	80.4
	W	6.4	55.5	52.3	91.9
2		12.7	54.4	74.5	91.9
		10.2	76.8	74.5	104.5
3		22	60.4	83.3	104.5
		24.8	69.3	83.8	104.5

P : pinion
W : wheel

Stress : 0.1 N/mm^2

Theoretical calculations have shown that the most important parameter is Hertzian stress which occurs on the gear teeth and could induce fast coating wear and scuffing.

2.3 Description of the Joint Test Machine (see Figure 3)

a) Joint Test Machine Objectives

The test machine, which consists of the electromechanical joint and an inertia simulation, has been designed to allow interchangeability of the electrical components while using the same joint. Several configurations are available for testing:

- Configuration 1: Brushless DC motor, angular potentiometer (output shaft) and optical encoder (input shaft)
- Configuration 2: Brushless DC motor, optical encoder for input and output angular position sensing
- Configuration 3: Stepper motor with the sensors of Configuration 2. This configuration is not presented in detail because some numerical problems must be resolved to achieve feedback law stability.

b) Test Machine Technological Definition (see Figure 4)

The choice of electrical components has been made with the main criteria, vacuum operation without significant outgassing. Also, bearing lubrication and materials have been selected to satisfy environmental conditions of low outgassing.

List of components:

- Brushless DC motor: SAGEM 23 MCM90, space-qualified
- Stepper motor SAGEM 23 PP, space-qualified
- Brake: Binder magnetic 86: 61104, vacuum rated only
- Optical encoder: Sopelem RI110: vacuum rated only

c) Inertia Simulator (see Figure 5)

The objective is to simulate an inertia of 800 Kg m^2 on the output of the joint shaft. Several solutions were examined. Step-up gearing with a tooth belt was chosen to minimize mass and reduce volume in the vacuum chamber. Moreover, it allows a good simulation of the robotic arm inertia parameters.

- Simulated inertia: 800 Kgm^2
- Step-up gearing ratio: 125
- Step-up gearing stiffness: 1950 Nm/Rad.

3. GEAR MATERIAL AND LUBRICATION PROCESSES

3.1 Material Trade-off

High contact stresses occur with the given requirements and lead to a material which provides good mechanical characteristics. These include yield strength, surface hardness, and contact pressure fatigue resistance. Good machinability is also required to obtain excellent geometric tolerances

Among different alloy and stainless steels, 35NCD16 steel was chosen, which has the following advantages:

- Air hardened, which produces minimum deformation
- Ease of plasma nitrided (if necessary)
- Use after tempering without other surface treatment
- Useful for heavy dynamic loads combined with fatigue, one of the best steels used in aircraft technology.

3.2 Lubrication Processes

In considering lubrication, the investigation was deliberately limited to dry lubricants. To ensure sufficient life and to avoid scuffing, a coating must be used which gives low friction coefficient and low wear rate.

Possibilities giving satisfaction in this case are:

- crystalline solids with lamellar structure (MoS_2)
- soft metals (Pb, Au, Ag)
- anti-wear ceramics (TiN, TiC)
- polymer materials (PTFE, polyamides, polyacetal)

To help choose the right solution, gears coated with different dry lubricants were tested on a "four square" (closed loop) gear test machine. These machines allow simulation of the speed and load environment of each reducer stage.

The selection criteria for the coatings are:

- no scuffing in ultravacuum
- low wear rate
- low friction coefficient
- no geometric modification during and after coating
- good adhesion between coating and substrate.

Five treatments were selected for preliminary experiments at atmospheric pressure. Those which gave better performance were later tested in a vacuum (10^{-7} Torr).

Descriptions of coatings, test machines and results in air were given in 1985 at the 2nd European Space Mechanisms and Tribology Symposium at Meersburg, Germany.

Performance classification is as follows:

	Heavy load Low speed	Medium load Medium speed
1	PTFE	PTFE
2	MoS_2	MoS_2
3	TiN	FeMoS
4	Ion nitriding	Ion nitriding
5	FeMoS	TiN

The underlined coatings give satisfactory results in air.

3.3 Vacuum Tests

In tests under vacuum, the field was narrowed to PTFE and MoS_2 for the final choice of coating (see Figure 6). The chronology of these tests was:

1) Running-in process with a small torque
2) Qualification test of 100 hours with the nominal torque
3) Qualitative examination of the teeth
4) Short test with step-by-step increasing torque from nominal to maximum value. Each step lasts five hours.
5) Endurance test of 100 hours with maximum torque to classify coatings and to evaluate their resistance under severe loading conditions.

In the case of medium speed (100 rev/min) and medium Hertzian pressure (450 N/mm^2), both coatings had satisfactory friction coefficient evolution, but PTFE provided less surface wear. In case of low speed (2 rev/min) and high Hertzian pressure (550 N/mm^2), only PTFE reached the end of the endurance test (84,000 revolutions) without damage.

It was not possible to estimate the real friction coefficient during this endurance test because of disturbances caused by debris located in the four-point angular contact ball bearings. Finally, PTFE performed best in vacuum and it had a rather good accommodation to misalignment. We finally chose it for the robotic joint application.

3.4 Robotic Joint Gears

The gears were tooled on a MIKRON milling machine. Then they were checked before and after PTFE deposition. Profile, lead, run-out, pitch deviation, and tooth thickness were controlled.

The ISO quality range after treatment was always better than or equal to 6, except for the internal ring whose quality was 7.

4. DYNAMIC ASPECTS OF THE JOINT

4.1 Feedback Loop Description

a) Configuration 1

The DC brushless motor operates as a servo actuator with an analog position feedback loop. The rotor angular position is sensed by an optical encoder, sampled and differentiated to obtain angular speed. A numerical speed loop is implemented to damp high frequency oscillations. The reducer output position is sensed by a potentiometer.

Functional Scheme

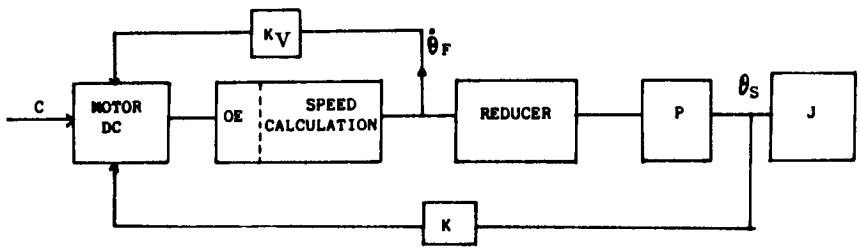

OE - Optical encoder
P - Potentiometer
J - Simulated inertia
K - Position gain
K_V - Speed gain

b) Configuration 2

For this case, the potentiometer is replaced by an optical encoder which senses the output angular position.

c) Configuration 3

This configuration uses a stepper motor with a specific dynamic control law. A torque feedback control law has been simulated, but the first experiments indicated some stability problems due to the numerical speed calculation.

This configuration is not considered as a nominal solution because of the feedback complexity. Dynamic analysis and electronic improvement have been performed to prove the feasibility of the law. The results of these studies and experiments will be presented at the symposium.

4.2 Servo Loop Definition

The dynamic system can be treated as a second-order problem if rotor inertia, reducer output inertia, and the electrical constant of the motor are neglected.

The differential equation is:

$$J_s \ddot{\theta}_s + \frac{K_v \dot{\theta}_s + K\theta_s}{T_a} = T_m - T_R$$

θ_S: Output position
N: Reducer ratio
K: Position gain
K_V: Speed gain
T_a: Control torque
T_m: Motor torque
T_R: Resisting torque
J_S: Output inertia

with the usual 2nd order servo parameters:

$$\frac{J_s}{K} = \frac{1}{\omega_N^2}$$ ω_N : Undamped eigenfrequency

$$\frac{2\zeta}{\omega_N} = \frac{K_v}{K}$$ ζ : Damping rate

$$\frac{1}{K} = G$$ G : Static gain

With ω_N = 1.125 Rad./sec and ζ = 1

K and K_V are calculated to be

$K = 1000$ Nm/Rad.
$K_V = 1800$ Nm/Rad./sec

These theoretical gains have been introduced in the experimental servo electronics. Some stability problems in the high frequency range limit speed gain efficiency.

The phenomena can be explained by the following considerations: In the backlash range, the load inertia changes between two extreme values: low rotor inertia and high simulated inertia. The digital tachometer encoder cannot track these rapid changes in motor rate without significant phase lag. Rate sampling precision is poor because the samping frequency is low (5 msec).

To improve the servo loop stability, it is possible to add a low-pass filter in series with the digital tachometer output. It appears that one of the best solutions is to use an analog tachometer for the high frequency range and a digital tachometer for the low frequency range. This mix of the two types of rate feedback provides the desired characteristics, while attenuating undesirable phenomena.

5. PROTOTYPE JOINT EXPERIMENTS

5.1 Philosophy of Testing

The purpose of the tests was to achieve confidence in the performance of the electromechanical joint under heavy loading and long operation in an ultravacuum environment.

The main objective was to assess the performance of the dry-lubricant gear reducer and electrical components. Backlash and friction coefficient evolution are the most important parameters which characterize reducer transmission.

During preliminary analysis, dynamic performance of the joint was evaluated using different types of feedback loop. The angular excursion law consists of large amplitude movements, small oscillations and locking phases. This is considered a good simulation of the approach and grappling sequence. All dynamic parameters are easily modified, utilizing a "menu" on a computer. The following parameters are automatically recorded: output angular position, motor position, winding intensity, and motor speed (deduced from sampled angular position (200 Hz)).

5.2 Parameter Measurements Before Endurance Tests

- Backlash

After assembly, it is easy to check the residual backlash by comparing the information from the two optical encoders when rotational direction is changed. However, before final assembly, backlash has been checked by measuring the axial displacement of a comparator placed on the output gear of the reducer, the motor being locked. The measured backlash in this case was:

$$j = 5 \times 10^{-4} \text{ Rad.} \simeq 1.7 \text{ Arc min}$$

- Friction Torque

Joint friction torque was measured with an angular dynamometer before final assembly with an inertia simulator. Two values were obtained by rotating the joint successively by each extremity. The results were similar ($T = 0.04$ Ncm), proving good joint reversibility.

The multiplier mechanism had an effective friction torque of 0.6 Ncm, but there is a dispersion in the results, depending on the belt tension. The global resisting torque was about 0.65 Ncm.

- Efficiency

At maximum speed and nominal torque, the motor efficiency is determined as follows:

$$\eta_M = \frac{T \times \omega}{U \times I}$$

T - Torque
I - Winding current
ω - Angular velocity
U - Voltage

$$\eta_M = \frac{\omega}{(R/K^2)T + \omega}$$

R - Winding resistance
K - Torque constant

R = 10.5 ohms
K = 0.06 Nm/A
T = 0.08 Nm

so that

$$\eta_M \simeq 0.04$$

When the inertia decreases, motor efficiency rises to 0.3. Measurement was made of the global mechanical efficiency of the joint with a constant resisting torque of 0.09 Nm. A torque of 0.042 Nm on the motor shaft was obtained.

Then,

$$\eta_G = \frac{T_M \ \omega_M}{T_R \ \omega_R}$$

T_M = Motor torque
T_R = Resisting Torque
ω_M = Motor speed
ω_R = Output speed

The multiplier efficiency was also measured and found to be $\eta = 0.85$. An estimate of the reducer efficiency is then

$$\eta_\eta = \frac{\eta_G}{\eta} = \frac{0.69}{0.85} = 0.81$$

This corresponds to $\eta = 0.93$ for each meshing gear.

- Stiffness

To ensure good locking stiffness, a steel housing was placed on the joint. The joint torsional stiffness was calculated with individual shaft and gear contributions. A value of $K \simeq 1 \times 10^5$ Nm/rad was obtained. This value was checked by measuring the angular difference between the two encoders under the following conditions: the brake was locked and the output inertia mass was loaded by a static torque.

With an 11.85 Nm applied torque, an angular difference of 0.03 deg was measured. Global stiffness was deduced from the previous results to be K 23,000 Nm/rad.

The inertia simulator stiffness has been calculated to be K 2,000 Nm/rad.

- Inertia

Assuming a geometric design for the mechanical parts, we have:

- Joint output inertia : 0.84 $m^2 kg$
- Multiplier inertia : 800 $m^2 kg$
- Motor shaft inertia : 0.8 $m^2 kg$
- Ratio I load / I motor : 1,000

5.3 Preliminary Joint Experiments

- Maximum Static Torque Specification

A 56 Nm static torque was put on the joint using weights with the electromagnetic brake locked. One of the encoders was therefore fixed and the other rotated from 0 deg to 0.13 deg which confirmed the above stiffness value of about 25,000 Nm/rad. This test was repeated ten times without any angular position modification, thus demonstrating good behavior of the loaded gears and brake.

- Magnetic Brake Test

The brake was locked and the motor reversed from clockwise maximum torque to counterclockwise maximum torque. The motorshaft encoder was monitored to detect any rotation. No movement was observed.

In a second test, the brake was released for seven hours, which requires application of constant input voltage. Subsequently, after switching off the input voltage, the brake did not relock for several minutes. The reason for this may be the high temperature under vacuum, which increases the distance between the magnetic parts of the brake.

- Maximum Torque Motor Test

For this test, the output part of the joint was locked onto the housing and the motor driven from "0" to maximum current (0.17 Nm) with a linear rise during two minutes. This was repeated twenty times in succession. The motor was found reliable.

5.4 Endurance Tests

For all experiments, the minimum vacuum was 10^{-6} Torr, and was performed with a 600 ℓ/sec RIBER ion pump.

- Running in Process

With thick PTFE films (6 μm), the running-in process is very important. A low Hertzian pressure and small angular acceleration of 20 deg/sec (i.e., 1.52 Nm output torque was chosen. For run-in, the output gear was rotated 80 revolutions (40 clockwise and 40 counterclockwise).

- Cyclic Test Description

Two standard movements were recorded, one for large angular displacement with maximum dynamic performance and the other for large angular displacement combined with small oscillations to simulate a final capture.

The first standard movement, which is called A, consists of an angular excursion of 170 deg at the output of the joint. It begins with an accelerated phase (= 130 deg/sec , T = 10 Nm), followed by a constant angular rate of 500 deg/sec and finally, a decelerated phase with the same dynamic parameters. Then the joint comes back to the initial position with the same displacement law.

The second standard movement, B, has the same angular excursion and the same maximum angular rate, but the acceleration is limited to 65 deg/sec. Before coming back, four sinusoidal oscillations with a 1 deg amplitude are imposed on the joint.

- Endurance Test Procedure

The joint was tested with 1100 cycles of the A program (34 hours) and 1600 of the B program (87 hours), corresponding to a total of 121 hours lifetime.

The number of cyclic loads reached by each gear tooth was:

- Third stage internal ring : 5400
- Third stage pinion : 32700
- Second stage wheel : 32700
- Second stage pinion : 165600
- First stage wheel : 165600
- First stage pinion : 1987200

The average torques which were applied to the gear teeth are shown in Figure 7.

- Parameter Control

Each standard cycle was divided into several phases depending on the driving law. For each phase, a reference clock time was defined at which the position and angular rate parameters were automatically recorded by a computer program.

The program calculates, for these times, the difference between the theoretical position and the effective position of the joint and the difference between angular position at the ends of the joint. After analyzing 120 cycles, the program draws the evolution curves of the parameters and calculates the mean value and standard deviation for each one.

The following curves depict joint parameter fluctuations:

- Static position error: (Θoutput - Θtheoretical at t = 0) (see Figure 8)
- Dynamic error, recorded for the accelerated phase (see Figure 9)
- Output angular rate (see Figure 10)
- (Θoutput - Θinput x R(Ratio)): backlash variation, machined-gear-tooth deviation, and elastic deformation due to the load (see Figure 11).

- Backlash Evolution

Several measurements of backlash were performed during the lifetime tests. The final value, after 121 hours, is j = 1.8 arc/min (Figure 12). Thus, no significant evolution could be detected. Backlash evolution is representative of output gear wear. However, it is not possible to draw any conclusions about the wear of the other gear stages.

- Friction Coefficient Evolution

An 8 gm weight is sufficient to move the joint (T $\simeq$ 0.5 Ncm). On the other hand, the minimum motor voltage to start the joint is 0.42V, i.e., T = 0.75 cmN. These values are similar and no evolution could be detected.

- Gear Tooth Examination

The gear housing has some circular holes that allow direct examination of gear teeth with an endoscopic cane. Unfortunately, it is possible to observe only the second stage of the reducer. The teeth looked polished, almost brilliant, near the top, and it appears that the two mat blue-gray extremeties of the pinion were never in contact after 120 hours of running. If the results of checking (wear and surface inspection) and the functional performances (output backlash, resistant torque, efficiency) are all found to be in accordance with the specifications, the endurance test duration will be increased to 150 hours of running in ultravacuum. A discussion of the final results will be presented at the symposium.

CONCLUSIONS

These robotic joint endurance experiments are a good simulation of the orbital mission. The tests have confirmed behavior of the components after three months under vacuum and 121 hours working time, except for the brake which showed some problems due to increased temperature.

The feasibility of a robotic joint of 150 mm diameter and 100 mm length, with 10 Nm dynamic output torque and 60 Nm static torque, has been demonstrated for more than 100 hours lifetime with dry lubrication. The backlash and friction torque stability indicate a potential increased lifetime without significant damage.

Some improvements in the feedback law must be implemented in the future to take into account high frequency resonance problems, inertia simulator stiffness effects and the effect of backlash.

Although the new torque requirements of the Hermes telemanipulator arm are much higher than for the joint discussed in this paper, it seems that a joint with force capability in the range 10 to 20 Nm could have several applications in orbital station manipulators.

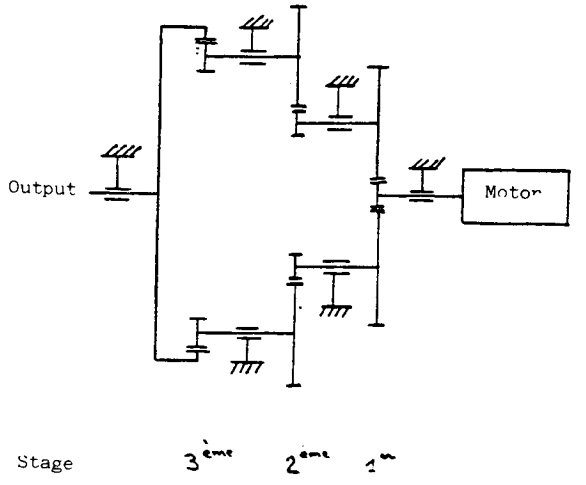

Figure 1. Gear box description

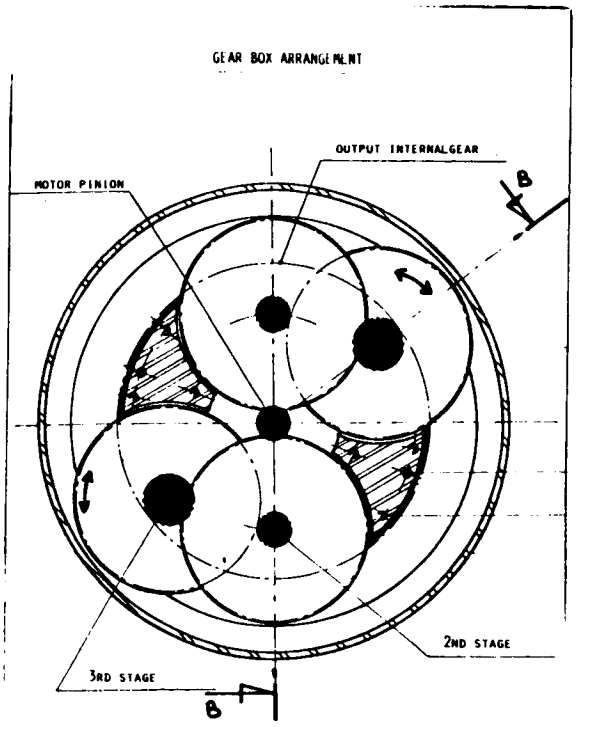

Figure 2. Gear box arrangement

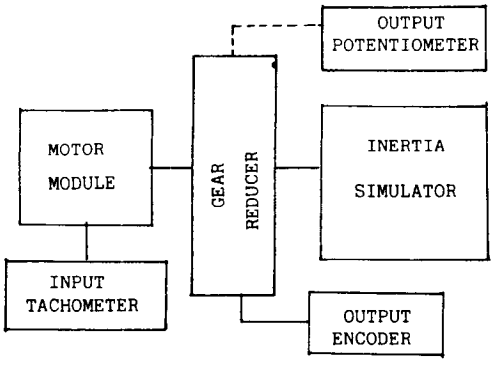

Figure 3. Joint prototype functionnal definition

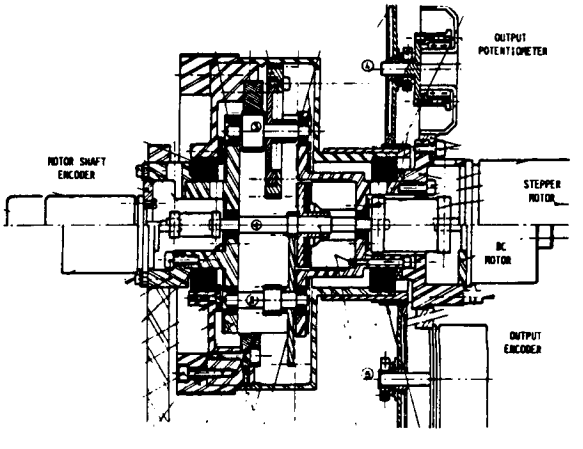

Figure 4. Prototype technological definition joint

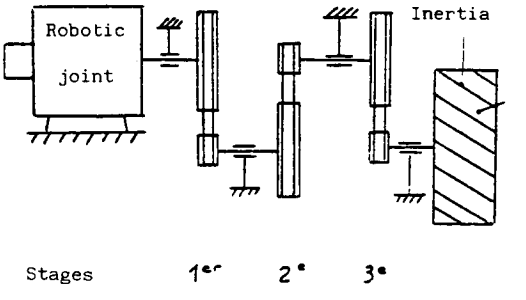

Figure 5. Inertia simulator

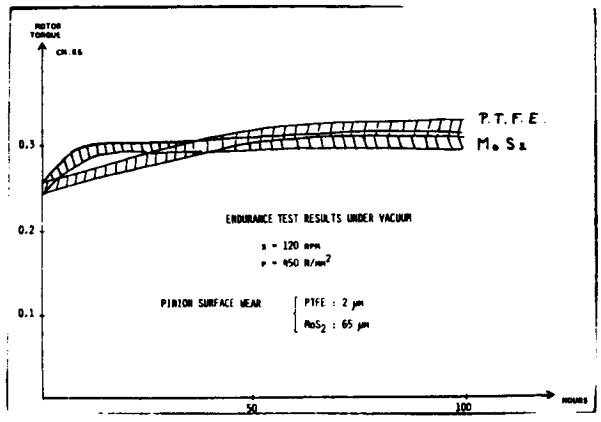

Figure 6. Endurance tests MOS2/PTFE

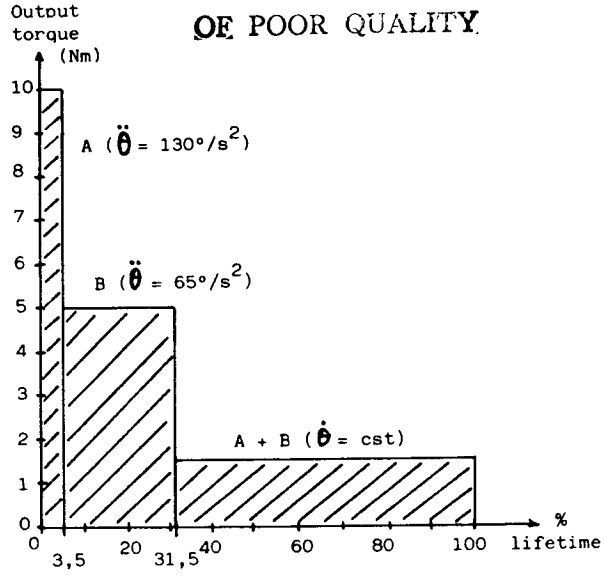

Figure 7.

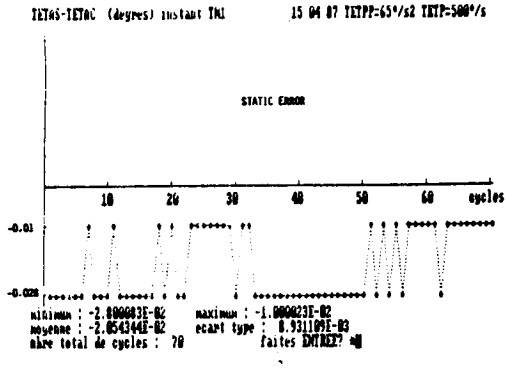

Figure 8. Static position error

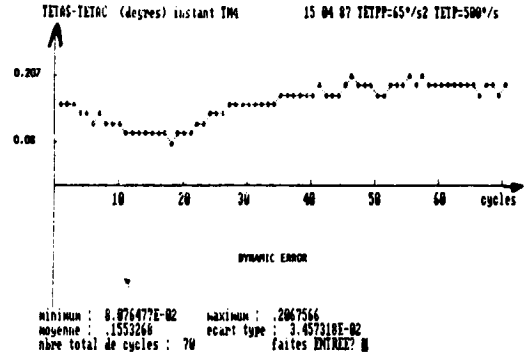

Figure 9. Dynamic error

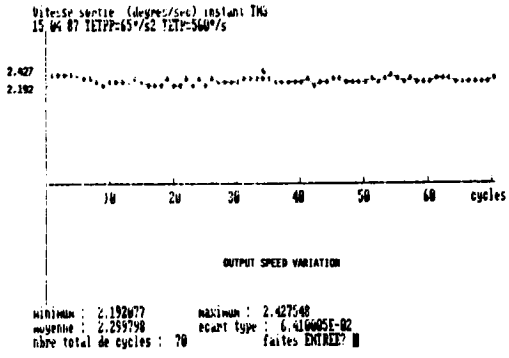

Figure 10. Output speed variation

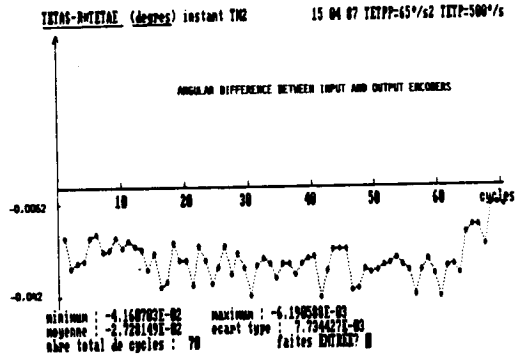

Figure 11. Backlash variation

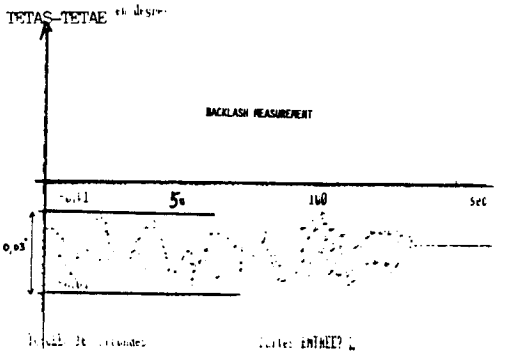

Figure 12. Backlash measurement